Self-Assembly

Deutsche Ausgabe: DOI: 10.1002/ange.201501081
Internationale Ausgabe: DOI: 10.1002/anie.201501081

Beyond Molecules: Mesoporous Supramolecular Frameworks Self-Assembled from Coordination Cages and Inorganic Anions**

Dong Luo, Xiao-Ping Zhou, and Dan Li**

Abstract: *Biological function arises by the assembly of individual biomolecular modules into large aggregations or highly complex architectures. A similar strategy is adopted in supramolecular chemistry to assemble complex and highly ordered structures with advanced functions from simple components. Here we report a series of diamond-like supramolecular frameworks featuring mesoporous cavities, which are assembled from metal-imidazolate coordination cages and various anions. Small components (metal ions, amines, aldehydes, and anions) are assembled into the hierarchical complex structures through multiple interactions including covalent bonds, dative bonds, and weak C–H···X (X = O, F, and π) hydrogen bonds. The mesoporous cavities are large enough to trap organic dye molecules, coordination cages, and vitamin B_{12}. The study is expected to inspire new types of crystalline supramolecular framework materials based on coordination motifs and inorganic ions.*

Chemists try to mimic and understand biological processes through designing and synthesizing progressively complex supramolecules and studying their advanced functions.[1,2] This mimicry is inspired by the highly complex and hierarchical structures of biological systems which express functions that are reckoned to arise from the combination of a myriad of weak interactions. For example, the quaternary structures of proteins are assembled from individual protein subunits, and new and advanced biological functions emerge from the higher-order structures. The individual subunits cannot exhibit the same biological functions without forming the higher-order structures. Remarkable success has been made by chemists through combining small molecules or ions together by using supramolecular approaches, for example, molecular machines[2] and huge assembled cages,[3–5] however, the level of complexity is still poor compared with biological systems.[6] To reach higher-order supramolecular architectures similar to biological systems, multiple interactions need to be synchronized to yield a synergistic effect.[7,8] The typical examples are polypeptides, in which covalent amino acid chains can fold to afford secondary order (α-chain or β-chain) and further self-organize into higher-order architectures through hydrogen bonding and hydrophobic/hydrophic interactions.

Metal coordination cages (or capsules, polyhedrons) have been widely investigated for their bionic feature, structural beauty, and potentially advanced applications (e.g. stabilization of reactive species,[9,10] recognition,[11,12] and catalysis[13,14]). Close attention has focused on how to assemble a desired cage with a certain geometry and size and to explore its inner cavities (e.g. host–guest chemistry); however, approaches for organizing cages into more complex or architecturally controlled frameworks through supramolecular interactions to achieve new advanced functions are still unusual.[15,16] In the study of metal–organic frameworks (MOFs), few chemists employ metal coordination cages as building blocks to assemble porous materials.[17–19] Here we describe the solvothermal subcomponent self-assembly of metal-imidazolate coordination cages, which are further assembled hierarchically with anions to yield supramolecular frameworks. Each hierarchical architecture is assembled from small components (metal ions, amines, aldehydes, and anions; Figure 1) through multiple interactions including covalent bonds, dative bonds, and weak C–H···X (X = O, F, and π) hydrogen bonds. The supramolecular frameworks with giant cavities of mesoporous size are capable of taking up large

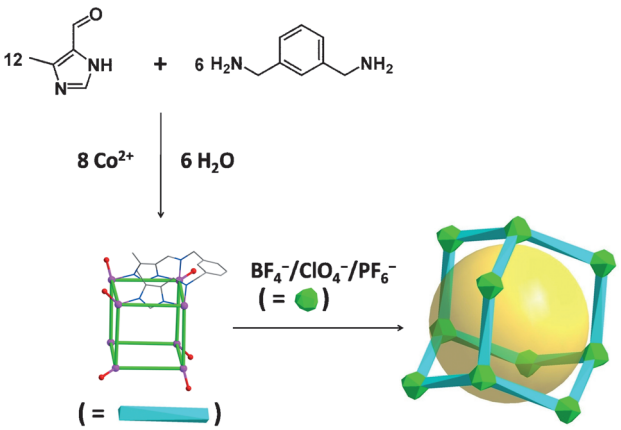

Figure 1. Illustration of the hierarchical self-assembly of the supramolecular framework. The big yellow ball represents the cavity in the framework; color codes: Co pink, O red, C gray, N blue; H atoms are omitted for clarity.

[*] D. Luo, Prof. Dr. X.-P. Zhou, Prof. Dr. D. Li
Department of Chemistry and Key Laboratory for Preparation and Application of Ordered Structural Materials of Guangdong Province, Shantou University
Guangdong 515063 (P. R. China)
E-mail: zhouxp@stu.edu.cn
dli@stu.edu.cn

[**] This work is financially supported by the National Basic Research Program of China (973 Program, 2012CB821706 and 2013CB834803), the National Natural Science Foundation of China (91222202, 21171114, 21101103, and 21371113), Guangdong Natural Science Funds for Distinguished Young Scholar, (2014A030306042), The Training Program for Excellent Young College Teachers of Guangdong Province, and Shantou University.

Supporting information for this article is available on the WWW under http://dx.doi.org/10.1002/anie.201501081.

molecules (an organic dye, metal coordination cages, or the biomolecule vitamin B_{12}), and thus a procedure has been developed in which aggregation gives rise to a desired function.

Solvothermal subcomponent self-assembly is a feasible approach to synthesize metal coordination cages and infinite polymeric compounds (e.g. MOFs).[20–22] The reactions of 5-methyl-4-formylimidazole and *m*-xylylenediamine with the cobalt(II) salts $Co(ClO_4)_2{\cdot}6H_2O$, $Co(BF_4)_2{\cdot}6H_2O$, and $Co(BF_4)_2{\cdot}6H_2O$-KPF_6 under solvothermal conditions (see the Supporting Information for details) resulted in three isomeric compounds (**1**, **2**, and **3**, respectively). Single crystals of **1**, **2**, and **3** were obtained directly in high yields. It is noteworthy that all the reagents are commercially available and the syntheses are simple, which further demonstrates the power of solvothermal subcomponent self-assembly.

Single-crystal X-ray diffraction analyses showed that **1**, **2**, and **3** feature identical hierarchical supramolecular architectures that crystallize in the same cubic $Fd\bar{3}$ space groups with giant unit cell volumes (127730(7), 127464(5), and 130189(5) $Å^3$ for **1**, **2**, and **3**, respectively). As an example, the structure of **1** will be described in detail. As shown in Figure 1, the cobalt ions were coordinated by the bisimidazole ligands H_2L (H_2L = 1,3-bis[(5-methyl-1*H*-imidazol-4-yl)methyleneaminomethyl]benzene) to form an eight-nucleus cubic cage, similar to our previously reported cubic Ni-imidazolate cage.[21] The bisimidazole ligand L was formed in situ by the condensation of 5-methyl-4-formylimidazole and *m*-xylylenediamine, as was further evident from the IR spectrum (C=N absorbance band around 1610 cm^{-1}, see Figure S1 in the Supporting Information). Two cobalt ions in the cubic cage adopt octahedral coordination geometry, and each one is chelated by three ligands L, with Co–N bond lengths ranging from 1.907(6) to 1.944(6) Å. The shorter Co–N bonds indicate that the octahedral Co center has a valence of +3,[23] and the Co^{III} state is probably obtained by the oxidization of Co^{II} by oxygen during the reaction. Interestingly, the two octahedral Co^{III} ions have opposite asymmetric arrangements of the coordinated ligand (Δ and Λ, respectively, see Figure S2 in the Supporting Information), and as a whole the Co-imidazolate cage is achiral. The other six Co ions in the cage adopt distorted square-pyramidal geometries and each Co center is coordinated by four nitrogen atoms and one oxygen atom (from water), with Co–N bond lengths ranging from 2.016(6) to 2.227(6) Å, which are clearly longer than the Co^{III}–N bonds, and thus indicate these Co ions have a valence of +2. The Co-imidazolate cubic cage of **1** represents an unusual example of a coordination cage containing mixed-valence metal ions in markedly different coordination geometries. Similar to the cubic Ni-imidazolate cages, the edge lengths in the Co-imidazolate cubic cage are also around 6.1 Å (6.053–6.181 Å, Co···Co distance). A guest water molecule fills the hole of the cage (see Figure S3 in the Supporting Information).

The eight-nucleus Co-imdazolate cage is positive and has a valence of +6, which is balanced by six anions (ClO_4^-, BF_4^-, PF_6^- for **1**, **2**, and **3**, respectively). However, only 3.5 ClO_4^-, 0.5 BF_4^-, and 3.5 PF_6^- can be determined crystallographically for the Co-imdazolate cages in **1**, **2**, and **3**, respectively. Normally, balance ions exist randomly in a crystal lattice around the ionic complexes (sometimes partial ions may not be found by crystallographic study), and are usually underemphasized. Amazingly, the anions in **1**, **2**, and **3** play a critical role in the further assembly of the cages into a higher-order supramolecular network. As shown in Figure 2b, the cubic Co-imidazolate cages are assembled

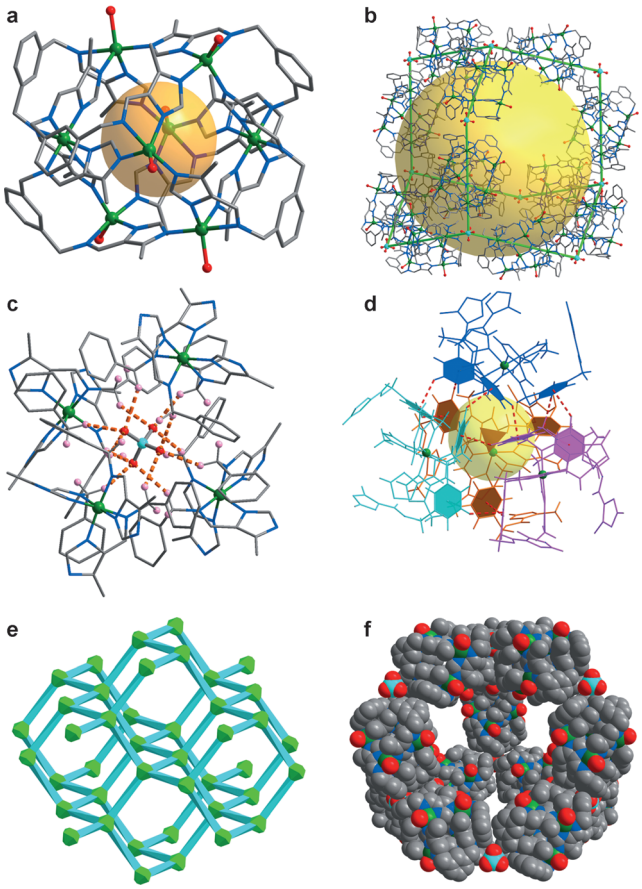

Figure 2. Illustration of the X-ray crystal structure of **1**: a) cubic eight-nuclear Co-imidazolate cage (the orange ball represents the inner cavity); b) supramolecular network formed through assembling the cage with ClO_4^- (the yellow ball represents the large cavity); c) the ClO_4^- ion is surrounded by four cages through C–H···O interactions (indicated by red dashed lines); d) C–H···π interactions between four cages (indicated by red dashed lines, the yellow ball represents the cavity, and the triangle represents the ClO_4^-); e) diamond topology (the cyan rods represent the cage, and the green polyhedra represent ClO_4^-); f) space-filling structure of a "diamond unit" showing a large cavity; color codes for elements: Co green, C gray, N blue, O red, Cl cyan, H pink (highlighted in c).

together by ClO_4^- in **1**, and further aggregate together in a high order. Each ClO_4^- ion is surrounded by four cages with a T_4 symmetry (see below), and each cage interacts with two ClO_4^- ions. Similar cases are found in **2** and **3** for BF_4^- and PF_6^-, respectively.

The unconventional and weak C–H···X (X = O, N, F, and π) hydrogen bonds commonly exist in artificial molecular architectures and biologic systems, and play important roles in crystal engineering and anion recognition,[24–26] inducing

(hydro)gelation,[27] and stabilizing protein structures and quasicrystals.[28,29] As a result of the C–H···X hydrogen bonds being weak, they always act as a supportive interaction rather than as a predominant one to direct the assembly. In **1**, the ClO_4^- ion in the crystal lattice is located in a hydrophobic pore surrounded by four Co-imidazolate cages, and forms C–H···O hydrogen bonds (H···O distance of about 2.657 Å) with the C–H proton of methanediyl from the ligands of the cages (Figure 2c). Although a C–H···O hydrogen bond is weak, twelve hydrogen bonds between each ClO_4^- and the methanediyl C–H groups should synergistically enhance the interactions between ClO_4^- and the cationic cages. In addition, the electrostatic interactions between the positive cages and negative ClO_4^- ion also probably help strengthen the connections. The C–H···O hydrogen bonds probably guide the aggregation of four Co-imidazolate cages to form the pore, which acts as a supramolecular host for a ClO_4^- ion (Figure 2d). Careful examination identified C–H···π interactions (H···π 2.689 Å, or edge-to-face π-π interactions) between benzyl groups from different cages (Figure 2d). There are also twelve C–H···π interactions to further stabilize the cage–anion aggregation. Similar phenomena happened in **2** and **3**, where BF_4^- and PF_6^- ions were located in the center of the pore of four cages, respectively. Twelve C–H···F hydrogen bonds and twelve C–H···π interactions exist in each host–guest system of the cages and BF_4^-/PF_6^-.

The assembly of ClO_4^- and Co-imidazolate cages leads to the formation of an extended diamond supramolecular network[30,31] (Figure 2e) in which the ClO_4^- ions act as 4-connected nodes and the cage acts as a linker. As a consequence of the relatively large size of the Co-imidazolate cage (2.0 nm length circumscribed) and the non-interpenetrated structure, the framework of **1** is highly porous (Figure 2b,f and see Figure S4 in the Supporting Information), and the potential solvent-accessible void volume is 90082.9 $Å^3$ in one unit cell, with 70.5% checked by PLATON. The cavity is filled by remaining anions and solvent molecules of *N*,*N*-diethylformamide (DEF) and water. Notably, the distance between antipodal oxygen atoms (binding H_2O) in one diamond unit of **1** is 37.7 Å (see Figure S5 in the Supporting Information), and the diagonal distance of the pore aperture is about 23.6 Å, which clearly show that the cavity is of mesoporous scale. A similar large pore size is also observed in both **2** and **3**. The large pore size in **1**, **2**, and **3** is comparable to those in mesoporous MOF materials.[32–34] To the best of our knowledge, **1**, **2**, and **3** represent uncommon examples of unconventional hydrogen-bonded networks with mesoporous cavities of previously unattained sizes.

As a result of the weak C–H···X interactions and highly porous properties, crystals of **1**, similar to protein crystals, are unstable in air and lose crystallinity quickly, as shown in the powder X-ray diffraction patterns (see Figure S6 in the Supporting Information). The low N_2 adsorption capacities (about 20.0 $cm^3 g^{-1}$ at $P/P_0 = 0.9$ and 77 K) further suggested that the mesoporous hydrogen-bonded framework easily collapsed (see Figure S8 in the Supporting Information). However, the crystal of **1** is stable in its saturated mother liquid, water, and ethanol solution. The stability of **1** in water and ethanol was monitored by single-crystal X-ray diffractions, and the diffraction quality of the crystals was still good after 72 h (see Figures S9 and S10 in the Supporting Information). Inclusion experiments of large organic and inorganic molecules (dyes and metal coordination cages), and biomolecules (vitamin B_{12} and small proteins) inside the pores of crystals **1** were carried out to assess the possible mesoporous porosity. Typically, crystals of **1** were immersed in an aqueous solution containing the particular large molecules to be included. Our trials demonstrate that some large molecules, including dyes, metal coordination cages, and vitamin B_{12}, can be incorporated into **1**, whereas protein cannot.

Dye molecules with various charges and shapes were selected for the inclusion experiments (see Figure S11 in the Supporting Information): Fluorescein disodium salt (Fl^{2-}), Acid Fuchsin (AF^{2-}), Methyl Orange (MO^-), Neutral Red (NR^0), Sudan 1 ($Sd1^0$), and Methylene Blue (MlB^+). Fresh crystals of **1** (15.0 mg) were immersed in an aqueous solution of dye (10.0 mL and concentration: $[Fl^{2-}] = [AF^{2-}] = [MO^-] = [NR^0] = 1 \times 10^{-4}$ M and $[MlB^+] = 5 \times 10^{-5}$ M, respectively) over a period of about 30 h. The amount of dye molecules in the supernatant was measured by UV/Vis spectrophotometry (characteristic absorbance: Fl^{2-} 493 nm, AF^{2-} 547 nm, MO^- 465 nm, NR^0 524 nm, and MlB^+ 664 nm). As shown in Figure 3a (and see Figure S12 in the Supporting Information), the plots of the dye concentrations with time clearly show a continuous decrease in the amount of anionic dye molecules (Fl^{2-}, AF^{2-}, and MO^-), and an invariability for those of neutral NR^0 and cationic MlB^+. These results preliminarily show that anionic dye molecules can be selectively included in the cavities of **1**, whereas cationic molecules cannot (dye NR^0 is hydrolyzed and becomes cationic in water). The charge selectivity was further proved by immersing crystals of **1** into a solution containing both Fl^{2-} and MlB^+. The green supernatant of the dye mixture (vial 3 in the inset of Figure 3b) turned blue (vial 4) and the UV/Vis spectra clearly show that only anionic Fl^{2-} is selectively included in crystals **1** (Figure 3b). Sudan 1 ($Sd1^0$) was chosen to test the possibility of the inclusion of neutral dye molecules into the cavities of **1** in an ethanol solution. The solution color change and the UV/Vis spectral trace indicated that the neutral dye cannot be trapped by **1** (see Figure S13 in the Supporting Information). Therefore, the experiments solidly demonstrated that mesoporous **1** can selectively upload anionic dye molecules.

The reversibility of the trap and release has practical importance such as for use in drug delivery. To test the reversibility and recyclability, crystals of **1** with included MO^- were immersed in the same volume of a solution containing $NaClO_4$. The solution turned from colorless back to orange (see Figure S14 in the Supporting Information), thus indicating that ClO_4^- replaced MO^- in the mesoporous framework **1** (see also Figure S15 in the Supporting Information for spectral traces). In the absence of ClO_4^-, the released dye content in the MO^- inclusion solution stayed at almost zero. As the ClO_4^- concentrations increase, the amount of released MO^- increases (see Figure S16 in the Supporting Information). The UV/Vis measurement showed that the release of MO^- was about 80% after two replacement processes ($[ClO_4^-] = 0.2$ M and 51 h). Such an ion-exchange and release

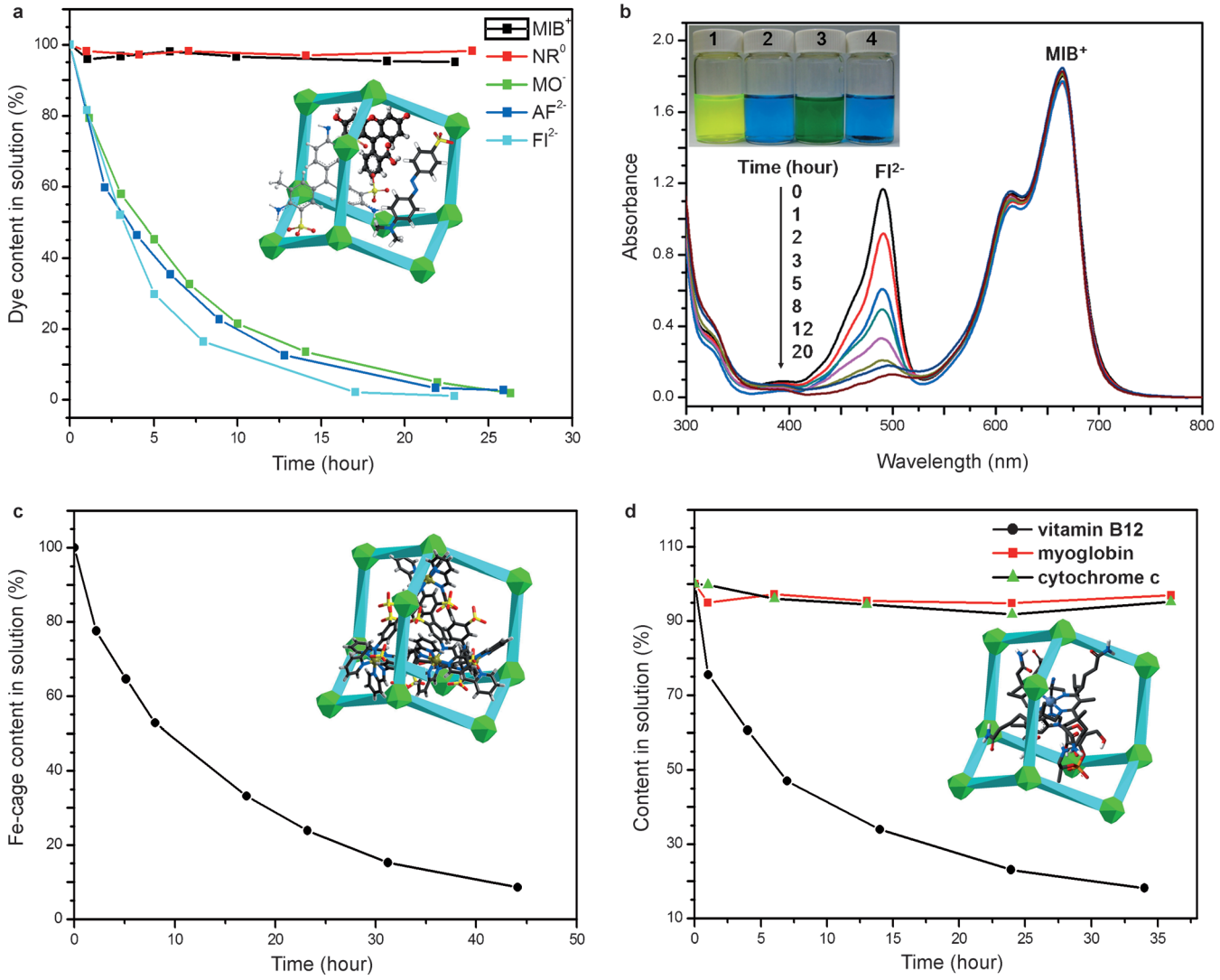

Figure 3. Inclusion studies of selected large molecules in **1**: percentage of dye (a), Fe coordination cage (c), and vitamin B_{12} and proteins (d) remaining in the solution as determined by the UV/Vis absorbance at a selected wavelength over time. The inset figures illustrate the inclusion complexes for each study. b) Selective inclusion of anionic dye molecules: UV/Vis spectra of a Fl^{2-} and MIB^{+} mixture in the presence of **1** (monitored over time). The photograph (insets) of vials shows the solution colors: vial 1: Fl^{2-}, vial 2: MIB^{+}, vial 3: Fl^{2-}/MIB^{+} mixture before inclusion, and vial 4: Fl^{2-}/MIB^{+} mixture after inclusion.

process was performed for three continuous cycles (see Figure S17 in the Supporting Information), and the process is reversible with no apparent drop in the ion-exchange capacity. Crystals of **1** remain transparent after three recycles, and look the same as the original samples (see Figure S19 in the Supporting Information). A single-crystal X-ray diffraction measurement study showed an identical unit as that of the original one of **1** (see Figure S20 in the Supporting Information), which indicates **1** is robust in the reversible dye trapping and release process in water.

The dye molecules are smaller than 2.0 nm. To assess the mesoporous properties of **1**, larger molecules were required. A reported tetrahedral Fe coordination cage $[NMe_4]_4Fe_4L_{imine}$ (L_{imine} = 4,4′-di(pyridin-2-ylmethyleneamino)biphenyl-2,2′-disulfonate; see Figure S21 in the Supporting Information) was selected because of its large size (2.2 nm), anionic nature, and water solubility.[35] The same experiment as with the anionic dye molecules was carried out by immersing crystals of **1** in the aqueous solution of the Fe coordination cage. The UV/Vis spectra and the color change of the solution clearly showed that Fe cages are also successfully exchanged into cavities of crystals of **1** (see Figure 3c and see Figure S22 in the Supporting Information), which probably form a complicate and unique cage in a cage-network clathrate. The inclusion of Fe coordination cages was further evident by inductively coupled plasma atomic emission spectrometry (ICP-AES) measurements showing a Fe/Co molar ratio of 1:4.8. This positive result illustrates the mesoporous cavities (>2.0 nm) in **1**. After the inclusion process, crystals of **1** turn a dark red but are still crystalline (see Figure S23 in the Supporting Information). Single-crystal X-ray diffraction measurements showed a unit cell which was identical with that of the original in **1** (see Figure S24 in the Supporting Information). Unfortunately, the diffraction quality was not

good enough to refine the crystal structure. To further test the capability of **1** to trap large molecules, the biomolecules vitamin B_{12} (cyanocobalamin) and small proteins (myoglobin and cytochrome c) were used. Similar procedures as above were used for the inclusion experiments in **1**. The fading of the red color of the supernatant and the decrease in the absorbance band at 361 nm in the UV/Vis spectra showed that the large biomolecule vitamin B_{12} can be trapped by crystals of **1** (Figure 3d, and see Figure S27 in the Supporting Information). A positive Cotton effect was observed in the CD spectrum of crystals of **1** that trapped vitamin B_{12}, and the peak position is identical with that of vitamin B_{12} (see Figure S28 in the Supporting Information), further confirming the successful uptake of vitamin B_{12} by **1**. In contrast, the invariable color of the supernatant and UV/Vis spectra (Figure 3d, and see Figures S33 and S34 in the Supporting Information) suggest that the small proteins myoglobin and cytochrome c cannot be included into the cavities of **1**, probably because of their large size and ease of unfolding (vitamin B_{12}: 27 Å, myoglobin: $21 \times 35 \times 44$ Å, cytochrome c: 31 Å).

Crystals **1**, **2**, and **3** are soluble in certain organic solvents (e.g. *N*,*N*-dimethylformamide (DMF) and dimethyl sulfoxide (DMSO)), which makes it very simple to test the regeneration, re-use, and recognition of other anions by the Co-imidazolate cage. Crystals of **1**, **2**, and **3** can be easily regenerated by diffusing ethyl ether slowly into DMF solutions of the crystals. Treatment of a DMF solution of **2** with an excess of $LiNO_3$ in DMF and slow diffusion of ethyl ether into the mixture solution lead to the formation of crystals **4**. Compound **4** crystallizes in a hexagonal $R\bar{3}$ space group, and contains two types of cubic Co-imdazolate cages (for details of the crystal structure see Figures S35 and S36 in the Supporting Information). The nitrate anions do not act as nodes to connect the Co-imdazolate cages through C–H···O hydrogen bonds, but act as substitutions to replace the coordinated water molecules. Trials using tetraethylammonium chloride gave compound **5** in which Cl^- ions replace the coordinated water molecules (for details of the crystal structure see Figures S37 and S38 in the Supporting Information), similar to that in **4**. Our experiments reveal that a large spherical shape with a weak coordination ability (such as ClO_4^-, BF_4^-, and PF_6^-) is suitable for interacting with Co-imidazolate cages to form mesoporous supramolecular frameworks, whereas simple anions such as NO_3^- and Cl^- cannot.

In summary, a series of mesoporous supramolecular frameworks were successfully prepared in one-pot reactions from cobalt cations, amines, aldehydes, and anions. The frameworks were constructed from Co-imidazolate cages and anions through covalent bonds, dative bonds, and weak C–H···X hydrogen bonds, and can efficiently trap large dye molecules, coordination cages, and the biomolecule vitamin B_{12}. The unit cells of the mesoporous supramolecular networks are close to those of diamond-like protein crystals,[36] which demonstrates the strategy of assembling large coordination cages into a hierarchical architecture. The results represent an efficient approach for mimicking a natural process. It is anticipated that a mesoporous supramolecule constructed from large aggregates of ordered structures will open up a general avenue for using such similar strategies and provide a potential platform for obtaining advanced crystalline materials.

Keywords: coordination cages · hydrogen bonds · imidazole · self-assembly · supramolecular frameworks

How to cite: *Angew. Chem. Int. Ed.* **2015**, *54*, 6190–6195
Angew. Chem. **2015**, *127*, 6288–6293

[1] V. Serreli, C.-F. Lee, E. R. Kay, D. A. Leigh, *Nature* **2007**, *445*, 523–527.
[2] B. Lewandowski, G. De Bo, J. W. Ward, M. Papmeyer, S. Kuschel, M. J. Aldegunde, P. M. E. Gramlich, D. Heckmann, S. M. Goldup, D. M. D'Souza, A. E. Fernandes, D. A. Leigh, *Science* **2013**, *339*, 189–193.
[3] Q. F. Sun, J. Iwasa, D. Ogawa, Y. Ishido, S. Sato, T. Ozeki, Y. Sei, K. Yamaguchi, M. Fujita, *Science* **2010**, *328*, 1144–1147.
[4] B. Olenyuk, M. D. Levin, J. A. Whiteford, J. E. Shield, P. J. Stang, *J. Am. Chem. Soc.* **1999**, *121*, 10434–10435.
[5] Y. Liu, C. Hu, A. Comotti, M. D. Ward, *Science* **2011**, *333*, 436–440.
[6] R. F. Service, *Science* **2005**, *309*, 95–95.
[7] X. Yan, S. Li, T. R. Cook, X. Ji, Y. Yao, J. B. Pollock, Y. Shi, G. Yu, J. Li, F. Huang, P. J. Stang, *J. Am. Chem. Soc.* **2013**, *135*, 14036–14039.
[8] X. Yan, S. Li, J. B. Pollock, T. R. Cook, J. Chen, Y. Zhang, X. Ji, Y. Yu, F. Huang, P. J. Stang, *Proc. Natl. Acad. Sci. USA* **2013**, *110*, 15585–15590.
[9] P. Mal, B. Breiner, K. Rissanen, J. R. Nitschke, *Science* **2009**, *324*, 1697–1699.
[10] H. Takezawa, T. Murase, M. Fujita, *J. Am. Chem. Soc.* **2012**, *134*, 17420–17423.
[11] R. A. Bilbeisi, J. K. Clegg, N. Elgrishi, X. d. Hatten, M. Devillard, B. Breiner, P. Mal, J. R. Nitschke, *J. Am. Chem. Soc.* **2012**, *134*, 5110–5119.
[12] I. A. Riddell, M. M. J. Smulders, J. K. Clegg, Y. R. Hristova, B. Breiner, J. D. Thoburn, J. R. Nitschke, *Nat. Chem.* **2012**, *4*, 751–756.
[13] D. Fiedler, D. H. Leung, R. G. Bergman, K. N. Raymond, *Acc. Chem. Res.* **2005**, *38*, 349–358.
[14] M. D. Pluth, R. G. Bergman, K. N. Raymond, *Acc. Chem. Res.* **2009**, *42*, 1650–1659.
[15] W. Wei, W. Li, X. Wang, J. He, *Cryst. Growth Des.* **2013**, *13*, 3843–3846.
[16] Z. Zhang, L. Wojtas, M. J. Zaworotko, *Chem. Sci.* **2014**, *3*, 849–1252.
[17] J.-R. Li, D. J. Timmons, H.-C. Zhou, *J. Am. Chem. Soc.* **2009**, *131*, 6368–6369.
[18] F. Nouar, J. F. Eubank, T. Bousquet, L. Wojtas, M. J. Zaworotko, M. Eddaoudi, *J. Am. Chem. Soc.* **2008**, *130*, 1833–1835.
[19] Y. Yan, S. Yang, A. J. Blake, M. Schröder, *Acc. Chem. Res.* **2014**, *47*, 296–307.
[20] J. R. Nitschke, *Acc. Chem. Res.* **2007**, *40*, 103–112.
[21] X.-P. Zhou, Y. Wu, D. Li, *J. Am. Chem. Soc.* **2013**, *135*, 16062–16065.
[22] Y. Wu, X.-P. Zhou, J.-R. Yang, D. Li, *Chem. Commun.* **2013**, *49*, 3413–3415.
[23] M. H. Alkordi, J. L. Belof, E. Rivera, L. Wojtas, M. Eddaoudi, *Chem. Sci.* **2011**, *2*, 1695.
[24] G. R. Desiraju, *J. Am. Chem. Soc.* **2013**, *135*, 9952–9967.
[25] A. S. Degtyarenko, E. B. Rusanov, A. Bauza, A. Frontera, H. Krautscheid, A. N. Chernega, A. A. Mokhir, K. V. Domasevitch, *Chem. Commun.* **2013**, *49*, 9018–9020.
[26] G. R. Desiraju, *Acc. Chem. Res.* **2002**, *35*, 565–573.

[27] C. Rest, M. J. Mayoral, K. Fucke, J. Schellheimer, V. Stepanenko, G. Fernández, *Angew. Chem. Int. Ed.* **2014**, *53*, 700 – 705; *Angew. Chem.* **2014**, *126*, 716 – 722.
[28] A. Senes, I. Ubarretxena-Belandia, D. M. Engelman, *Proc. Natl. Acad. Sci. USA* **2001**, *98*, 9056 – 9061.
[29] N. A. Wasio, R. C. Quardokus, R. P. Forrest, C. S. Lent, S. A. Corcelli, J. A. Christie, K. W. Henderson, S. A. Kandel, *Nature* **2014**, *507*, 86 – 89.
[30] A. Yamamoto, T. Hamada, I. Hisaki, M. Miyata, N. Tohnai, *Angew. Chem. Int. Ed.* **2013**, *52*, 1709 – 1712; *Angew. Chem.* **2013**, *125*, 1753 – 1756.
[31] M. J. Zaworotko, *Chem. Soc. Rev.* **1994**, *23*, 283 – 288.
[32] G. Férey, C. Mellot-Draznieks, C. Serre, F. Millange, J. Dutour, S. Surblé, I. Margiolaki, *Science* **2005**, *309*, 2040 – 2042.
[33] Y. K. Park, S. B. Choi, H. Kim, K. Kim, B.-H. Won, K. Choi, J.-S. Choi, W.-S. Ahn, N. Won, S. Kim, D. H. Jung, S.-H. Choi, G.-H. Kim, S.-S. Cha, Y. H. Jhon, J. K. Yang, J. Kim, *Angew. Chem. Int. Ed.* **2007**, *46*, 8230 – 8233; *Angew. Chem.* **2007**, *119*, 8378 – 8381.
[34] W. Xuan, C. Zhu, Y. Liu, Y. Cui, *Chem. Soc. Rev.* **2012**, *41*, 1677 – 1695.
[35] P. Mal, D. Schultz, K. Beyeh, K. Rissanen, J. R. Nitschke, *Angew. Chem. Int. Ed.* **2008**, *47*, 8297 – 8301; *Angew. Chem.* **2008**, *120*, 8421 – 8425.
[36] N. Dotan, D. Arad, F. Frolow, A. Freeman, *Angew. Chem. Int. Ed.* **1999**, *38*, 2363 – 2366; *Angew. Chem.* **1999**, *111*, 2512 – 2515.
[37] CCDC 1035116, 1035117, 1035118, 1035119, 1035120 contain the supplementary crystallographic data for this paper. These data can be obtained free of charge from The Cambridge Crystallographic Data Centre via www.ccdc.cam.ac.uk/data_request/cif.

Received: February 4, 2015
Published online: April 7, 2015

